Anti-VEGFA Therapy Reduces Tumor Growth and Extends Survival in a Murine Model of Ovarian Granulosa Cell Tumor[1,2]

Mayra Tsoi*, Marie-Noëlle Laguë*, Alexandre Boyer*, Marilène Paquet[†], Marie-Ève Nadeau[‡] and Derek Boerboom*

*Centre de Recherche en Reproduction Animale, Faculté de Médecine Vétérinaire, Université de Montréal, St-Hyacinthe, Québec, Canada; [†]Comparative Medicine and Animal Resources Centre, McGill University, Montréal, Québec, Canada; [‡]Département des Sciences Cliniques, Faculté de Médecine Vétérinaire, Université de Montréal, St-Hyacinthe, Québec, Canada

Abstract

Although angiogenesis has been proposed as a therapeutic target for the treatment of ovarian granulosa cell tumor (GCT), its potential has not been evaluated in controlled studies. To do so, we used the $Pten^{tm1Hwu/tm1Hwu}$; $Ctnnb1^{tm1Mmt/+}$;$Amhr2^{tm3(cre)Bhr/+}$ (PCA) mouse model, which develops GCTs that mimic the advanced disease in women. A monoclonal anti–vascular endothelial growth factor A (VEGFA) antibody was administered weekly to PCA mice beginning at 3 weeks of age. By 6 weeks of age, anti-VEGFA therapy significantly decreased tumor weights relative to controls ($P < .05$) and increased survival, with all treated animals but none of the controls surviving to 8 weeks of age. Analyses of PCA tumors showed that anti-VEGFA treatment resulted in significant decreases in tumor cell proliferation and microvessel density relative to controls ($P < .05$). However, treatment did not have a significant effect on apoptosis or tumor necrosis. The VEGFA receptor 2 (VEGFR2) signaling effector p44/p42 mitogen-activated protein kinase (MAPK), whose activity is associated with cell proliferation, was significantly less phosphorylated (i.e., activated) in tumors from the treated group ($P < .05$). Conversely, no significant difference was found in the activation of protein kinase B, a VEGFR2 signaling effector associated with cell survival. Together, these results suggest that anti-VEGFA therapy is effective at inhibiting GCT growth in the PCA model and acts by reducing microvascular density and cell proliferation through inhibition of the VEGFR2-MAPK pathway. Findings from this preclinical model therefore support the investigation of targeting VEGFA for the adjuvant treatment of GCT in women.

Translational Oncology (2013) 6, 226–233

Introduction

The granulosa cell tumor (GCT) is the most prevalent of the sex cord/stromal subgroup of ovarian tumors in women and is thought to represent up to 5% of all ovarian cancers [1–4]. Although GCT is often characterized as a low-grade malignancy [5,6], approximately 80% of patients with stage III or IV tumors die from recurrent disease [7]. Furthermore, a large proportion of patients develop recurrences as late as 40 years after the initial diagnosis and treatment [8], and therefore, fastidious long-term follow-up is required [1,3,9]. Despite the importance and insidiousness of GCT, it has received very little attention from the cancer research community, particularly relative to the more prevalent ovarian epithelial tumors. Perhaps as a consequence of this, the development of therapeutic approaches for GCT has lagged

well behind other forms of ovarian cancer. Initial management of GCTs involves cytoreductive surgery, and in cases of recurrence or advanced disease, adjuvant treatment is frequently attempted [1,3–5,9,10]. These

adjuvant treatments have included chemotherapy, radiotherapy, hormonal therapy, and more recently, anti-angiogenic therapy [1,3,4,9,10]. Studies aiming to evaluate current adjuvant treatment protocols for GCTs in women have been limited to retrospective studies and case reports, and no well-designed randomized studies have been conducted to determine if any such regimen actually confers a survival advantage [4,5,11–13].

Among the potential therapeutic targets that have been proposed for the development of novel treatments for GCT [14–16], angiogenesis would appear to be particularly promising. GCTs are highly vascularized tumors, and angiogenesis is suspected to play an important role in their development and progression [4,17,18]. Vascular endothelial growth factor A (VEGFA) is a key mediator of angiogenesis and is implicated in endothelial cell proliferation, migration, survival, and vascular permeability [18–21]. VEGFA is overexpressed in 94% of GCTs [2], and its main receptor, VEGFR2, is expressed at high levels in 82% of primary and recurrent GCTs in both endothelial and granulosa cells [18]. VEGF was shown to be produced by endothelial as well as granulosa tumor cells [17]. In addition, VEGFA also has well-established pro-proliferative and cytoprotective functions in normal granulosa cells [22–24] and could therefore serve to promote GCT cell proliferation and suppress apoptosis, in addition to promoting angiogenesis. Collectively, these data suggest a very strong potential for VEGFA as a therapeutic target for GCT.

Avastin (bevacizumab) is a recombinant humanized monoclonal anti-VEGFA antibody that has received US Food and Drug Administration (FDA) approval for use in the treatment of metastatic colorectal cancer and non-squamous, non–small cell lung cancer in combination with chemotherapy [4,25–27], as well as metastatic renal cell carcinoma (combined with interferon-α) and glioblastoma (as a second-line treatment) [http://www.avastin.com/patient/index.html (accessed 30 May 2012)]. Whereas some reports have shown potential beneficial effects of bevacizumab in the treatment of ovarian epithelial cancer [28–30], very few studies have investigated its use in the treatment of GCT. Tao et al. [4] carried out a small retrospective case series and evaluated the clinical efficacy of bevacizumab with or without concurrent chemotherapy and found a response rate of 38% and a clinical benefit rate of 63%. This study was limited, however, by its retrospective nature, its small sample size, and the variation of treatments administered [4]. One case report [31] reports symptomatic improvement with bevacizumab combined with paclitaxel for the treatment of refractory GCT, while another case report [32] found no clinical improvement with bevacizumab for the first-line treatment of adult-type GCT. No prospective trial has been conducted to determine the efficacy of single-agent bevacizumab in the treatment of GCT.

A major factor that has impeded the development of novel therapeutic approaches for ovarian cancer (including GCT) has been the dearth of relevant preclinical animal models [10,33,34]. We have recently developed a genetically engineered mouse model, $Pten^{tm1Hwu/tm1Hwu}$; $Ctnnb1^{tm1Mmt/+}$;$Amhr2^{tm3(cre)Bhr/+}$ (PCA), in which the phosphoinositide 3-kinase (PI3K)/protein kinase B (AKT) is derepressed and the WNT/CTNNB1 pathway is constitutively activated specifically in granulosa cells [35]. PCA mice develop bilateral GCTs with 100% penetrance, perinatal onset, rapid growth, and many histopathologic features of the human disease [35,36]. Importantly, as for the advanced disease in women, PCA GCTs can form distant metastases and disseminate within the peritoneal cavity [35,36]. In this study, we therefore used the PCA preclinical model to perform the first controlled study to investigate the efficacy of anti-VEGFA therapy for the treatment of GCT disease. We hypothesized that intraperitoneal (i.p.) administration of anti-VEGFA antibody would effectively reduce tumor growth, reduce tumor vasculature, and increase tumor cell apoptosis, thereby improving survival in this murine model of GCT.

Materials and Methods

Animals and Treatments

PCA mice were obtained by selective breeding of the $Pten^{tm1Hwu}$, $Ctnnb1^{tm1Mmt}$, and $Amhr2^{tm3(cre)Bhr}$ parental strains, and genotypes were verified as previously described [35]. Tumor development in the PCA model follows a predictable course. At birth, all PCA mice display nests of dysplastic cells in both ovaries indicating that tumor growth is initiated perinatally. By 3 weeks of age, GCTs are already fully formed and continue to grow in a very rapid and aggressive fashion with abdominal distension becoming apparent by 5 weeks of age and extreme by 7 weeks. Death due to tumor-related causes inevitably occurs before 9 weeks of age [35,36]. PCA mice were administered anti-mouse VEGFA monoclonal antibody clone B20-4.1.1 (provided by Genentech, Inc, San Francisco, CA) by i.p. injection at 5 mg/kg (or 0.9% NaCl as a control) once a week beginning at 3 weeks of age. The mice were sacrificed at 3, 4, 5, 6, 7, and 8 weeks of age and their ovarian tumors, lungs, and abdominal organs were collected for subsequent use in immunohistochemistry, immunofluorescence, terminal deoxynucleotidyl transferase dUTP nick end labeling (TUNEL) assays, Western blot analysis, and histopathology. To evaluate the effects of variable doses, additional PCA mice received 2.5, 5, or 10 mg/kg of anti-VEGFA antibody weekly i.p. beginning at 3 weeks of age until 6 weeks of age, at which point mice were sacrificed and their tumors and organs were collected as described above ($n = 8$–16 mice/treatment/time point). Masses of tumors used in all analyses are indicated in Table W1.

All animal procedures were approved by the Institutional Animal Care and Use Committee of the University of Montreal and conformed to the Canadian Council on Animal Care Policy on Humane Care and Use of Laboratory Animals.

Immunohistochemistry and Immunofluorescence

Immunohistochemistry was performed on formalin-fixed, paraffin-embedded, 3-μm ovarian tumor sections ($n = 4$ mice/treatment/time point) using the VectaStain Elite Avidin-Biotin Complex Kit (Vector Laboratories, Inc, Burlingame, CA) as directed by the manufacturer. Sections were probed with proliferating cell nuclear antigen (PCNA) mouse monoclonal antibody (Cell Signaling Technology, Danvers, MA, Catalog No. 2586) as directed by the manufacturer, except incubation with the primary antibody (dilution of 1:2000) was performed for 30 minutes, and incubation with the secondary antibody (biotinylated anti-mouse reagent; Vector Laboratories, Inc; dilution of 1:250) was done for 10 minutes. Sections were also probed with phospho-p44/42 mitogen-activated protein kinase [MAPK; extracellular signal–regulated kinases 1 and 2 (ERK1/2)] (Thr202/Tyr204) (D13.14.4E) XP rabbit monoclonal antibody (mAb; Cell Signaling Technology; Catalog No. 4370, dilution of 1:200) as directed by the manufacturer. Staining was done using 3,3′-Diaminobenzidine Peroxidase Substrate Kit (Vector Laboratories, Inc) as directed by the manufacturer. To determine the number of PCNA-positive cells, four fields per tumor (one or two tumors per animal; at a ×630 magnification) were selected at random. From each field, cells were counted within a randomly selected circular area with a 90-μm diameter. For each tumor, percentage of PCNA-positive cells was calculated by dividing the sum

of PCNA-positive cells (from all fields) by the total number of cells. Sections of the same tumors stained with hematoxylin phloxine saffron stain (HPS) were also evaluated to quantify mitotic figures per ×400 field as a second measure of cell proliferative activity, as well as to estimate the extent of tumor necrosis. The area of coagulative necrosis (characterized by increased eosinophilia and glassy appearance of the area with loss of cellular details) was evaluated by light microscopy and was estimated for each tumor as a percentage of the total tumor cross section area. All slides were evaluated by a board-certified veterinary pathologist.

Immunofluorescence was performed on optimal cutting temperature compound (OCT)-embedded (Sakura Finetek USA, Inc, Torrance, CA) frozen ovarian tumors ($n = 4$ mice/treatment/time point). Samples were stored at –80°C until they were sectioned (4 μm) and allowed to dry for 5 hours. The slides were quick-fixed with 100% acetone (–20°C) for 20 seconds, wrapped in aluminum foil, and stored at –80°C. When ready, the slides were thawed at room temperature for 20 minutes, fixed with 100% acetone (–20°C) for 10 minutes, followed by 70% ethanol (–20°C) for 5 minutes. The slides were blocked with 10% goat serum diluted in phosphate-buffered saline (PBS) for 30 minutes and then probed with rat anti-mouse CD31 antibody (BD Biosciences, Franklin Lakes, NJ; Catalog No. 558736, dilution of 1:300, overnight at 4°C) and/or fluorescein-labeled *Lycopersicon Esculentum* (tomato) lectin (Vector Laboratories, Inc, Catalog No. FL-1171, dilution of 1:1000, 10 minutes at room temperature) diluted in 3% goat serum in PBS. The CD31-probed slides were incubated with the secondary antibody Alexa Fluor 594 goat anti-rat IgG (Invitrogen, Burlington, ON; Catalog No. A11007, dilution of 1:2000) for 1 hour at room temperature and diluted in 3% goat serum. The slides were washed with 1% Triton X-100 (Bioshop Canada, Inc, Burlington, ON) in PBS for 10 minutes and mounted with VECTASHIELD mounting medium for fluorescence with 4′,6-diamidino-2-phenylindole (DAPI; Vector Laboratories, Inc). To evaluate the amount of CD31 signal, five fields per tumor (at ×200 magnification) were selected at random and ImageJ software was used to quantify the area of signal emitted in each field. The evaluator was blinded with respect to the ages and treatments received. The double-labeled (CD31 + lectin) slides were used to confirm the specificity of endothelial cell staining.

TUNEL Assays

TUNEL assays were performed on formalin-fixed, paraffin-embedded, 3-μm ovarian tumor sections ($n = 4$ mice/treatment/time point) using the *In Situ* Cell Death Detection Kit, TMR red (Roche Diagnostics GmbH, Mannheim, Germany; Catalog No. 12156792910), according to the manufacturer's instructions. VECTASHIELD mounting medium for fluorescence with DAPI (Vector Laboratories, Inc) was used to mount the slides. To determine the number of positive cells for TUNEL, four fields per tumor (one or two tumors per animal; at ×630 magnification) were selected at random. Within each field, a circular area with a 90-μm diameter was chosen at random to count the number of TUNEL-positive cells. For each tumor, percentage of TUNEL-positive cells was calculated by dividing the sum of TUNEL-positive cells (from all fields) by the total number of cells. A normal healthy ovary containing atretic follicles was used as a positive control. The evaluator was blinded with respect to the ages and treatments received.

Western Blot Analysis

Tumor samples from 6-week-old *PCA* mice were used for Western blot analysis ($n = 4$ mice/treatment). Protein extracts were obtained using T-PER Tissue Protein Extraction Reagent and Halt Protease and Phosphatase Inhibitor Single-Use Cocktail (Thermo Fisher Scientific, Rockford, IL; Catalog Nos 78510 and 78442, respectively) as described by the manufacturer. Protein concentrations were quantified using the Bradford method. Samples (25 or 50 μg) were resolved on 7% to 12% sodium dodecyl sulfate–polyacrylamide gels and transferred to Hybond-P polyvinylidene difluoride (PVDF) Membrane (GE Amersham, Piscataway, NJ). Blots were probed with primary antibodies against p44/42 MAPK (ERK1/2) (137F5) rabbit mAb, phospho-p44/42 MAPK (ERK1/2) (Thr202/Tyr204) (D13.14.4E) XP rabbit mAb, AKT, phospho-AKT (Ser473) (587F11) mouse mAb, VEGF receptor 2 (55B11) rabbit mAb, phospho–VEGF receptor 2 (Tyr951) (15D2) rabbit mAb, phospho–VEGF receptor 2 (Tyr 1059) (D5A6) rabbit mAb (Cell Signaling Technology; Catalog Nos 4695, 4370, 9272, 4051, 2479, 4991, and 3817, respectively), and β-actin (C4) (Santa Cruz Biotechnology, Inc, Santa Cruz, CA; Catalog No. sc-47778) as directed by the manufacturers. The blots were incubated with enhanced chemiluminescence (ECL) peroxidase-labeled secondary antibodies (GE Amersham), and then ECL Plus Western blotting detection reagents (GE Amersham) were used to visualize the protein bands by chemiluminescence on high-performance chemiluminescence film (GE Amersham). The signal strengths were quantified using Kodak 1D v.3.6.5 software (Eastman Kodak Company, Rochester, NY).

Statistical Methods

Effects of antibody treatment on tumor size, cell proliferation, cell apoptosis, CD31 signal intensity, and VEGFA signaling pathway protein expression were analyzed by analysis of variance, followed by Newman-Keul or Dunnett post-test to identify differences between specific groups. $P < .05$ was considered statistically significant. Prism 4.0a software (GraphPad Software, Inc, San Diego, CA) was used for analysis.

Results

Anti-VEGFA Therapy Reduces Tumor Burden and Improves Survival in PCA Mice

To study the efficacy of anti-VEGFA therapy in the *PCA* model, mice were treated with anti-VEGFA antibody (5 mg/kg, i.p.) once a week beginning at 3 weeks of age. The mice were sacrificed at 3, 4, 5, 6, 7, and 8 weeks of age and their ovarian tumors and viscera were collected for analysis. A dose-response experiment was also conducted using 2.5, 5, and 10 mg/kg of anti-VEGFA, i.p., once a week, beginning at 3 weeks of age until 6 weeks of age, at which point the mice were sacrificed.

PCA mice treated with anti-VEGFA antibody in the dose-response trial demonstrated that significant effects on tumor burden were obtained at the 5 mg/kg dose, but no further benefit was obtained at 10 mg/kg (Figure 1*A*). In the time course trial, *PCA* mice showed significantly reduced ovarian tumor weights at 6 and 7 weeks of age relative to controls (Figure 1*B*). Importantly, anti-VEGFA treatment also extended the survival of treated animals. Whereas all animals treated with anti-VEGFA antibody survived up to 8 weeks of age, 27.8% ($n = 5$ of 18) of controls died before 7 weeks of age or had to be euthanized due to deteriorating health, and no control mice survived until 8 weeks of age (Figure 1*C*).

Anti-VEGFA Treatment Reduces Cell Proliferation but Does Not Affect Apoptosis in PCA GCTs

To determine the cause(s) of reduced GCT size in anti–VEGFA-treated *PCA* mice, cell proliferation was assessed by PCNA immunohistochemistry and by histologic analysis of mitotic figures. A significant
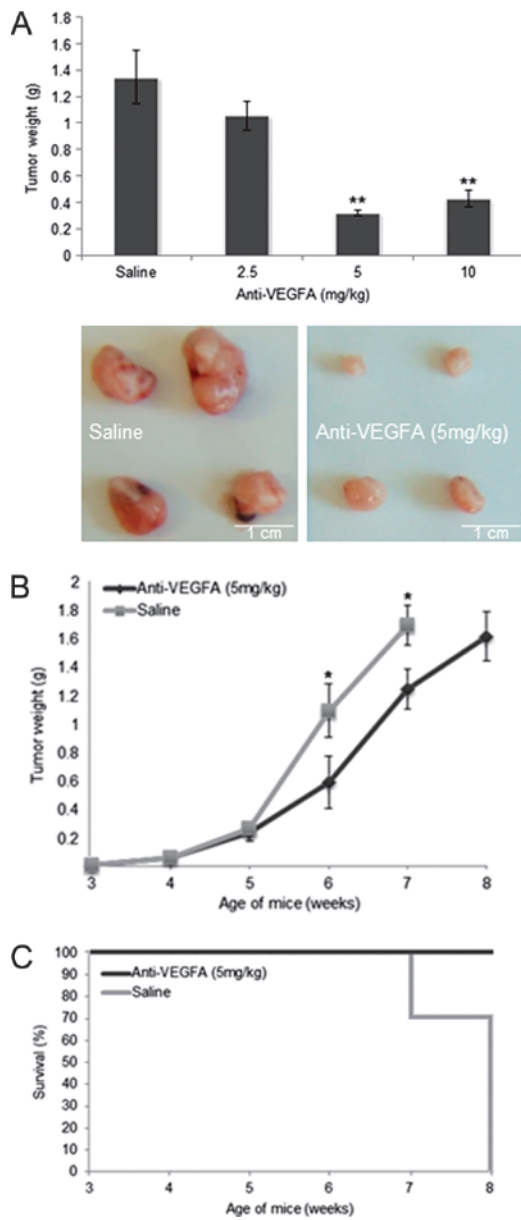
Figure 1. Anti-VEGFA antibody reduces tumor burden and improves survival of *PCA* mice with GCTs. (A) Effects of different doses of anti-VEGFA on tumor mass in 6-week-old *PCA* mice (n = 8–16 mice/treatment/time). Data are shown as means (columns) ± SEM (error bars). Significant difference from control (saline) is indicated with one (*P < .05) or two asterisks (**P < .01). Photographs of representative tumors are shown below the graph. (B) Time course of GCT mass with or without weekly anti-VEGFA treatment in *PCA* mice (n = 10–26 mice/treatment/time). (C) Survival curves indicating the proportion of experimental mice surviving at the indicated times (n = 4–18 mice/treatment/time). Anti–VEGFA-treated mice were sacrificed for humane reasons at 3 days past the 8-week time point.

decrease in the number of PCNA-positive cells was observed in the anti–VEGFA-treated group compared to the saline group at 6 weeks of age (Figure 2A). Likewise, fewer mitoses per high-power field were observed at 6 weeks of age in the anti–VEGFA-treated group (Figure 2B).

TUNEL assays were performed to determine if increased tumor cell apoptosis contributed to the decrease in tumor growth in anti–VEGFA-treated mice. No significant difference in the number of

TUNEL-positive cells in the anti–VEGFA-treated group compared to the saline group was observed at any age (Figure 3A). Likewise, although small foci of necrosis were observed in some tumors (particularly at 6 weeks), anti-VEGFA therapy did not increase the overall area of necrosis observed in histologic sections (Figure 3B).

Anti-VEGFA Treatment Significantly Reduces Tumor Microvessel Density in GCTs

To study the effects of anti-VEGFA antibody on angiogenesis in *PCA* GCTs, the tumor microvasculature was visualized by immunofluorescence using the endothelial cell marker CD31 (PECAM-1). Tumors from 6-week-old, anti–VEGFA-treated mice had a markedly lower microvessel abundance than saline-treated controls, with CD31 signal reduced by more than half in the 5 mg/kg group (Figure 4, A–C). Specificity of the CD31 signal for endothelial cells was confirmed by double labeling with tomato plant lectin (Figure 4D).
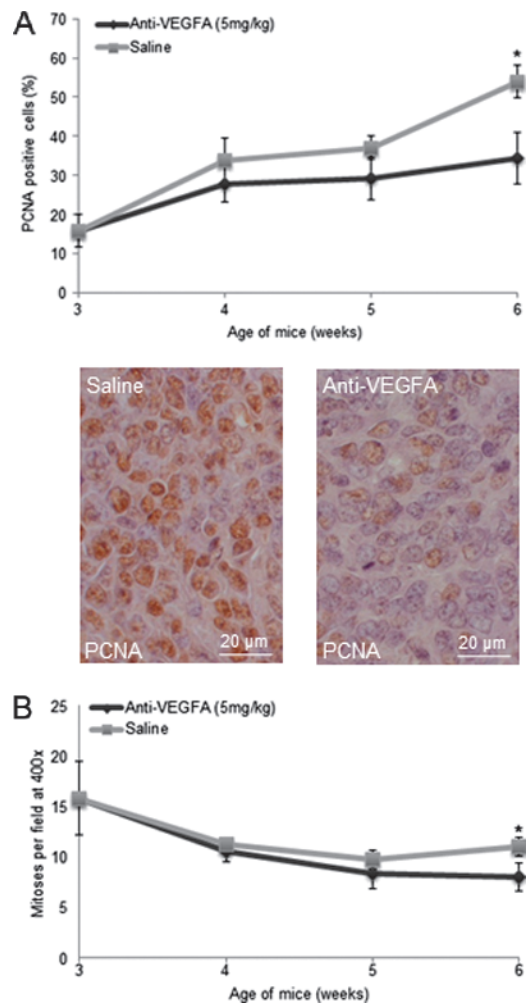

Figure 2. Anti-VEGFA antibody reduces cell proliferation in GCTs from *PCA* mice. (A) Graph depicting the proportion (as percentage) of PCNA-positive cells in *PCA* mice administered anti-VEGFA antibody or saline (control), n = 4 mice/treatment/time point. Representative photomicrographs of PCNA-stained tumors are shown below the graph at a ×630 magnification. (B) Evaluation of mitotic indices in the tumors described in A. Error bars = SEM. Significant difference from control (P < .05) is indicated with an asterisk.
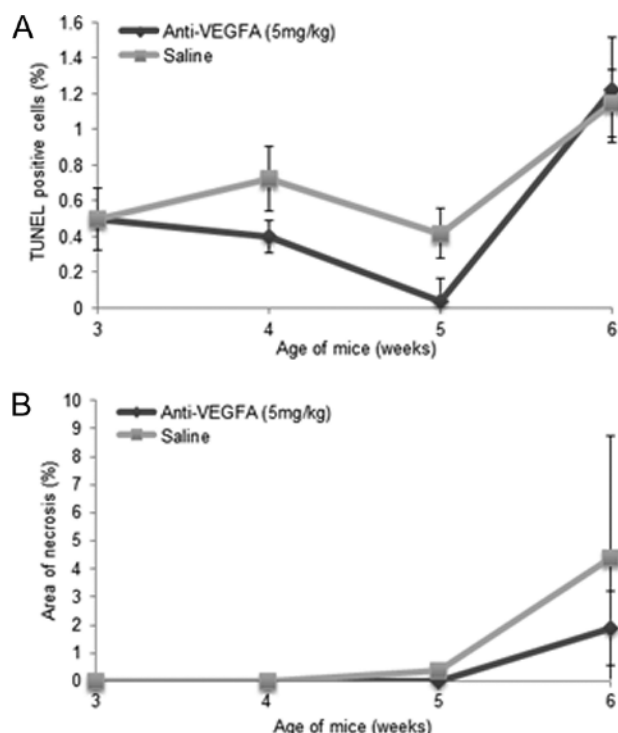
Figure 3. Anti-VEGFA antibody has no significant effect on apoptosis or tumor necrosis in GCTs from *PCA* mice. (A) Graph depicting the proportion (as percentage) of TUNEL-positive cells in *PCA* mice administered anti-VEGFA antibody or saline (control), $n = 4$ mice/treatment/time point. (B) Evaluation of extent of tumor necrosis (as percentage of total surface in histologic sections) in the tumors described in A. Error bars = SEM.

Intracellular Signaling Is Altered in Tumors from PCA *Mice Treated with Anti-VEGFA Antibody*

To identify potential alterations in intracellular signaling activity downstream of VEGFR2 caused by anti-VEGFA treatment, activity levels of the p44/42 MAPK (ERK1/2) and the PI3K/AKT signaling pathways were evaluated by Western blot analysis. Levels of phospho-p44/42 MAPK (Thr202/Tyr204) were significantly lower in GCTs from 6-week-old *PCA* mice that had received as little as 2.5 mg/kg of anti-VEGFA antibody, as was the ratio of phosphorylated-to-total p44/42 MAPK (Figure 5, *A* and *B*), indicative of decreased MAPK signaling activity. Immunohistochemistry was performed to determine the cell population(s) within the tumors in which this decrease occurred, which showed that granulosa, stromal, and endothelial cells (identified on the basis of morphologic characteristics) all appeared to be affected (Figure 5*C*).

Contrary to the MAPK pathway, no significant difference was found in the expression of AKT or phospho-AKT between the various anti–VEGFA-treated groups and the saline group (Figure 6, *A* and *B*), suggesting that activity of the PI3K/AKT pathway was not altered by treatment. Activation of VEGFR2 was also studied, but tyrosine phosphorylation of the receptor at sites 951 and 1059 could not be detected in either the anti–VEGFA-treated or the control groups (not shown).

Discussion

Few therapeutic options exist for advanced stage and recurrent GCT, and none of the widely used chemotherapeutic regimens has been

rigorously evaluated with regard to its effectiveness [11,13,37,38]. The development of validated adjuvant chemotherapies for GCT is therefore of paramount importance. Whereas angiogenesis (i.e., VEGFA) has been proposed as a therapeutic target for GCT [4,17,18,31,32], clinical investigations of anti-VEGFA therapies have so far been limited to small-scale retrospective studies and case reports and have yielded limited insight [4,31,32]. In this report, we used the recently developed *PCA* mouse model, which develops an ovarian cancer that mimics many of the histologic and biologic aspects of advanced human GCT [35,36], to investigate the efficacy of an anti-VEGFA antibody analogous to bevacizumab. Our results in this preclinical model clearly show that anti-VEGFA therapy extends survival and significantly slows tumor growth. These findings therefore support the prospective investigation of anti-VEGFA therapy for the adjuvant treatment of GCT in women.

Our findings indicate that the main mechanism by which the anti-VEGFA antibody slowed tumor growth was inhibition of tumor cell proliferation rather than induction of apoptosis. Proliferation was presumably inhibited, at least in part, by reduced microvessel density, resulting in decreased delivery of nutrients and growth factors to tumor
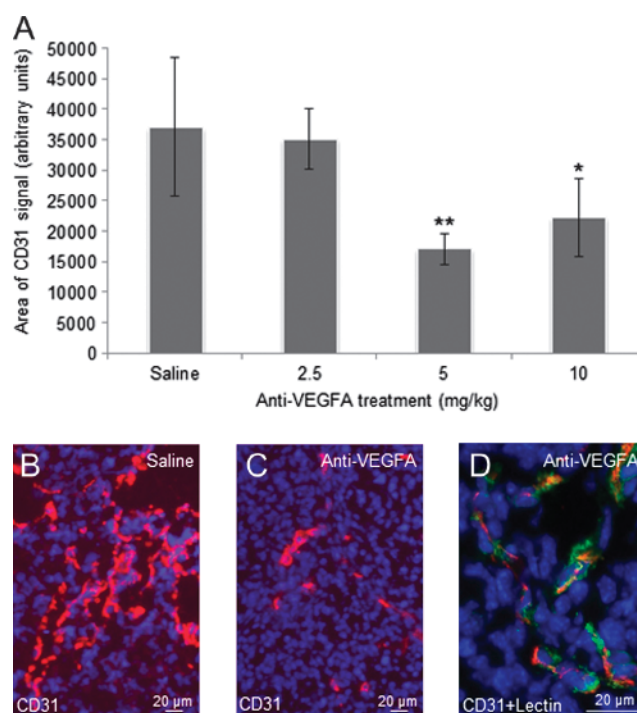

Figure 4. Anti-VEGFA antibody significantly reduces microvessel density in GCTs from 6-week-old *PCA* mice. (A) Graph depicting CD31 immunofluorescence signal strengths in GCTs from 6-week-old *PCA* mice that received the indicated treatments ($n = 4$ animals/treatment). Data are shown as means (columns) $\pm$ SEM (error bars). Significant difference from control (saline) is indicated with one (*$P < .05$) or two asterisks (**$P < .01$). (B) Representative photomicrograph (original magnification, $\times 200$) depicting CD31 fluorescent signal in the GCT of a 6-week-old *PCA* mouse. CD31-specific signal is red; nuclei are counterstained with DAPI (blue). (C) As per B, showing a tumor from an anti–VEGFA-treated mouse. (D) As per B, except endothelial cells were labeled with tomato plant lectin (green) in addition to CD31 immunolabeling; original magnification, $\times 630$. Overlap in lectin and CD31 signals appears yellow and confirms the specific labeling of endothelial cells by CD31.
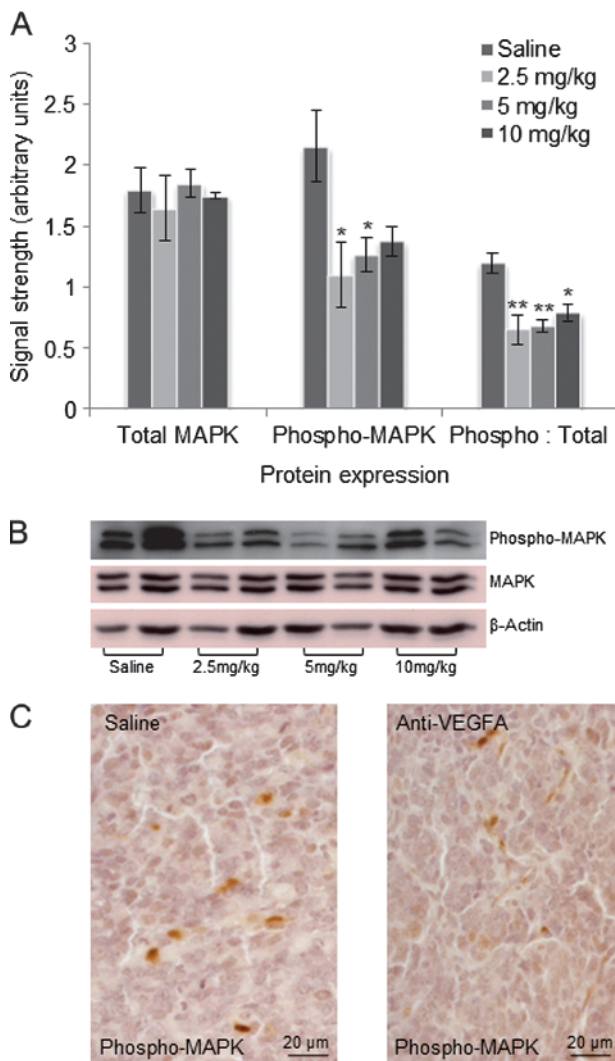
Figure 5. Anti-VEGFA antibody significantly reduces MAPK activation in GCTs from 6-week-old *PCA* mice. (A) Graph depicting expression of MAPK, phospho-MAPK, and phospho-MAPK/total MAPK ratio in tumors from 6-week-old *PCA* mice that received the indicated treatments. Data are densitometric quantification of signals obtained by Western blot analysis (*n* = 4 per treatment). Data are shown as means (columns) ± SEM (error bars). Significant difference from control (saline) is indicated with one (*P < .05) or two asterisks (**P < .01). (B) Representative Western blot images from the analyses shown in A (*n* = 2 samples/treatment). β-Actin was used as a loading control. (C) Immunohistochemical analysis of phospho-MAPK expression in tumors from 6-week-old *PCA* mice treated with saline control or anti-VEGFA (5 mg/kg); original magnification, ×400.

cells. However, our results also suggest that the anti-VEGFA therapy may have acted directly upon the tumor cells themselves to inhibit proliferation. Indeed, apparent lower levels of phosphorylation (i.e., activity) of the VEGFA receptor signaling effector MAPK were observed not only in endothelial cells but also in tumor cells from anti–VEGFA-treated mice. As MAPK signaling is thought to mediate the pro-proliferative actions of VEGFA [39,40], this suggests that the anti-VEGFA treatment acted to sequester pro-proliferative VEGFA from the tumor cells in the *PCA* model. This would be entirely consistent with the well-established role of VEGFA as a granulosa cell

growth factor in the context of normal ovarian follicle development [41,42] and would indicate that GCT cells retain a certain dependence on VEGFA as a proliferative signal even after oncogenic transformation. VEGFA also signals through the PI3K/AKT pathway, whose activity is associated with the antiapoptotic effects of VEGFA [43,44]. Anti-VEGFA therapy had no effect on tumor cell apoptosis in the *PCA* model and did not alter AKT phosphorylation (i.e., activity). VEGFA/AKT cytoprotective signaling would therefore not appear to be relevant to the pathogenesis of GCT, at least in the *PCA* model.

The effect of the anti-VEGFA antibody on GCT microvessel density in the *PCA* model concurs with findings from other studies that evaluated the effect of analogous anti-VEGFA antibodies on vascular growth. Korsisaari et al. [27] found a significant reduction in vessel density after 3 weeks of administration of anti-VEGFA mAb G6-31 in a murine model of intestinal adenoma. Likewise, Borgström et al. [45] found complete inhibition of angiogenesis in microtumors with administration of anti-VEGF antibody A4.6.1 in a tumor xenograft study of human prostate carcinoma. In past studies, anti-VEGFA therapy has been found to reduce tumor microvessel density, decrease permeability, increase tumor pericyte coverage, and stabilize the basement membrane, which all contribute to forming a more normalized tumor vasculature [46,47]. In consequence, tumor hypoxia and interstitial fluid pressure are reduced, which allows improved delivery of chemotherapy to the tumor, as observed in clinical trials [19,47,48]. If this holds true for GCT as well, another benefit of anti-VEGFA therapy may be to enhance the effects of other chemotherapeutic agents when used in the context of combinatorial therapy. The *PCA* mouse model
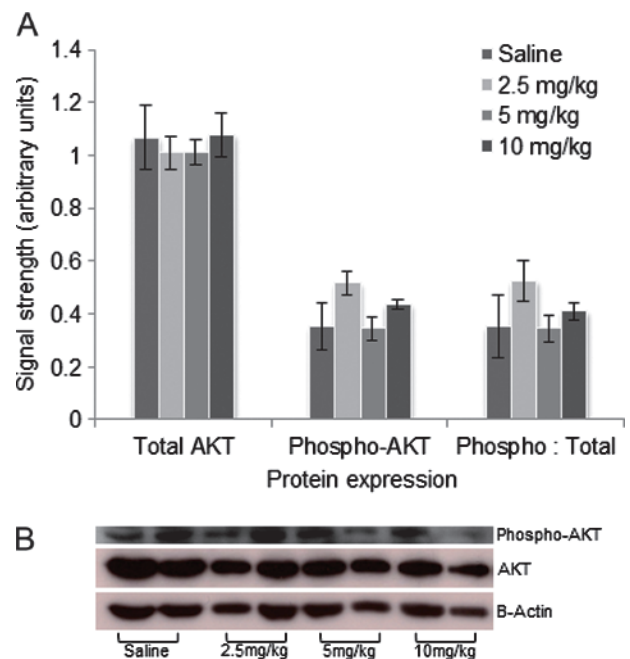

Figure 6. Anti-VEGFA antibody has no significant effect on AKT activation in GCTs from 6-week-old *PCA* mice. (A) Graph depicting expression of AKT, phospho-AKT, and phospho-AKT/total AKT ratio in tumors from 6-week-old *PCA* mice that received the indicated treatments. Data are densitometric quantification of signals obtained by Western blot analysis (*n* = 4 per treatment). Data are shown as means (columns) ± SEM (error bars). (B) Representative Western blot images from the analyses shown in A (*n* = 2 samples/treatment). β-Actin was used as a loading control.

may prove useful to test this hypothesis, as well as for the subsequent development of combinatorial treatment schemes.

In summary, this study shows that monotherapy with anti-VEGFA antibody is effective at suppressing tumor growth and extending survival in the *PCA* model of GCT. Targeting VEGFA reduced tumor cell proliferation and microvascular density, which could sensitize GCTs to the effects of other chemotherapeutic agents. On the basis of our results, we conclude that anti-VEGFA therapy shows great potential in the adjuvant treatment of GCT.

Acknowledgments

References

[1] Koukourakis GV, Kouloulias VE, Koukourakis MJ, Zacharias GA, Papadimitriou C, Mystakidou K, Pistevou-Gompaki K, Kouvaris J, and Gouliamos A (2008). Granulosa cell tumor of the ovary: tumor review. *Integr Cancer Ther* **7**, 204–215.

[2] Schmidt M, Kammerer U, Segerer S, Cramer A, Kohrenhagen N, Dietl J, and Voelker HU (2008). Glucose metabolism and angiogenesis in granulosa cell tumors of the ovary: activation of Akt, expression of M2PK, TKTL1 and VEGF. *Eur J Obstet Gynecol Reprod Biol* **139**, 72–78.

[3] Schumer ST and Cannistra SA (2003). Granulosa cell tumor of the ovary. *J Clin Oncol* **21**, 1180–1189.

[4] Tao X, Sood AK, Deavers MT, Schmeler KM, Nick AM, Coleman RL, Milojevic L, Gershenson DM, and Brown J (2009). Anti-angiogenesis therapy with bevacizumab for patients with ovarian granulosa cell tumors. *Gynecol Oncol* **114**, 431–436.

[5] Ayhan A, Salman MC, Velipasaoglu M, Sakinci M, and Yuce K (2009). Prognostic factors in adult granulosa cell tumors of the ovary: a retrospective analysis of 80 cases. *J Gynecol Oncol* **20**, 158–163.

[6] King LA, Okagaki T, Gallup DG, Twiggs LB, Messing MJ, and Carson LF (1996). Mitotic count, nuclear atypia, and immunohistochemical determination of Ki-67, c-myc, p21-ras, c-erbB2, and p53 expression in granulosa cell tumors of the ovary: mitotic count and Ki-67 are indicators of poor prognosis. *Gynecol Oncol* **61**, 227–232.

[7] Amsterdam A and Selvaraj N (1997). Control of differentiation, transformation, and apoptosis in granulosa cells by oncogenes, oncoviruses, and tumor suppressor genes. *Endocr Rev* **18**, 435–461.

[8] Hines JF, Khalifa MA, Moore JL, Fine KP, Lage JM, and Barnes WA (1996). Recurrent granulosa cell tumor of the ovary 37 years after initial diagnosis: a case report and review of the literature. *Gynecol Oncol* **60**, 484–488.

[9] Geetha P and Nair MK (2010). Granulosa cell tumours of the ovary. *Aust N Z J Obstet Gynaecol* **50**, 216–220.

[10] Jamieson S and Fuller PJ (2012). Molecular pathogenesis of granulosa cell tumors of the ovary. *Endocr Rev* **33**, 109–144.

[11] Sun HD, Lin H, Jao MS, Wang KL, Liou WS, Hung YC, Chiang YC, Lu CH, Lai HC, and Yu MH (2012). A long-term follow-up study of 176 cases with adult-type ovarian granulosa cell tumors. *Gynecol Oncol* **124**, 244–249.

[12] Malmstrom H, Hogberg T, Risberg B, and Simonsen E (1994). Granulosa cell tumors of the ovary: prognostic factors and outcome. *Gynecol Oncol* **52**, 50–55.

[13] Park JY, Jin KL, Kim DY, Kim JH, Kim YM, Kim KR, Kim YT, and Nam JH (2012). Surgical staging and adjuvant chemotherapy in the management of patients with adult granulosa cell tumors of the ovary. *Gynecol Oncol* **125**, 80–86.

[14] Fishman A, Kudelka AP, Tresukosol D, Edwards CL, Freedman RS, Kaplan AL, Girtanner RE, and Kavanagh JJ (1996). Leuprolide acetate for treating refractory or persistent ovarian granulosa cell tumor. *J Reprod Med* **41**, 393–396.

[15] Alhilli MM, Long HJ, Podratz KC, and Bakkum-Gamez JN (2012). Aromatase inhibitors in the treatment of recurrent ovarian granulosa cell tumors: brief report and review of the literature. *J Obstet Gynaecol Res* **38**, 340–344.

[16] Raspagliesi F, Martinelli F, Grijuela B, and Guadalupi V (2011). Third-line chemotherapy with tyrosine kinase inhibitor (imatinib mesylate) in recurrent ovarian granulosa cell tumor: case report. *J Obstet Gynaecol Res* **37**, 1864–1867.

[17] Farkkila A, Anttonen M, Pociuviene J, Leminen A, Butzow R, Heikinheimo M, and Unkila-Kallio L (2011). Vascular endothelial growth factor (VEGF) and its receptor VEGFR-2 are highly expressed in ovarian granulosa cell tumors. *Eur J Endocrinol* **164**, 115–122.

[18] Farkkila A, Pihlajoki M, Tauriala H, Butzow R, Leminen A, Unkila-Kallio L, Heikinheimo M, and Anttonen M (2011). Serum vascular endothelial growth factor A (VEGF) is elevated in patients with ovarian granulosa cell tumor (GCT), and VEGF inhibition by bevacizumab induces apoptosis in GCT *in vitro*. *J Clin Endocrinol Metab* **96**, E1973–E1981.

[19] Ho QT and Kuo CJ (2007). Vascular endothelial growth factor: biology and therapeutic applications. *Int J Biochem Cell Biol* **39**, 1349–1357.

[20] Greenberg JI and Cheresh DA (2009). VEGF as an inhibitor of tumor vessel maturation: implications for cancer therapy. *Expert Opin Biol Ther* **9**, 1347–1356.

[21] Ferrara N, Gerber HP, and LeCouter J (2003). The biology of VEGF and its receptors. *Nat Med* **9**, 669–676.

[22] Irusta G, Abramovich D, Parborell F, and Tesone M (2010). Direct survival role of vascular endothelial growth factor (VEGF) on rat ovarian follicular cells. *Mol Cell Endocrinol* **325**, 93–100.

[23] Kosaka N, Sudo N, Miyamoto A, and Shimizu T (2007). Vascular endothelial growth factor (VEGF) suppresses ovarian granulosa cell apoptosis *in vitro*. *Biochem Biophys Res Commun* **363**, 733–737.

[24] Greenaway J, Connor K, Pedersen HG, Coomber BL, LaMarre J, and Petrik J (2004). Vascular endothelial growth factor and its receptor, Flk-1/KDR, are cytoprotective in the extravascular compartment of the ovarian follicle. *Endocrinology* **145**, 2896–2905.

[25] Hurwitz H, Fehrenbacher L, Novotny W, Cartwright T, Hainsworth J, Heim W, Berlin J, Baron A, Griffing S, Holmgren E, et al. (2004). Bevacizumab plus irinotecan, fluorouracil, and leucovorin for metastatic colorectal cancer. *N Engl J Med* **350**, 2335–2342.

[26] Sandler A, Gray R, Perry MC, Brahmer J, Schiller JH, Dowlati A, Lilenbaum R, and Johnson DH (2006). Paclitaxel-carboplatin alone or with bevacizumab for non–small-cell lung cancer. *N Engl J Med* **355**, 2542–2550.

[27] Korsisaari N, Kasman IM, Forrest WF, Pal N, Bai W, Fuh G, Peale FV, Smits R, and Ferrara N (2007). Inhibition of VEGF-A prevents the angiogenic switch and results in increased survival of $Apc^{+/min}$ mice. *Proc Natl Acad Sci USA* **104**, 10625–10630.

[28] Burger RA, Brady MF, Bookman MA, Fleming GF, Monk BJ, Huang H, Mannel RS, Homesley HD, Fowler J, Greer BE, et al. (2011). Incorporation of bevacizumab in the primary treatment of ovarian cancer. *N Engl J Med* **365**, 2473–2483.

[29] Monk BJ, Han E, Josephs-Cowan CA, Pugmire G, and Burger RA (2006). Salvage bevacizumab (rhuMAB VEGF)-based therapy after multiple prior cytotoxic regimens in advanced refractory epithelial ovarian cancer. *Gynecol Oncol* **102**, 140–144.

[30] Richardson DL, Backes FJ, Seamon LG, Zanagnolo V, O'Malley DM, Cohn DE, Fowler JM, and Copeland LJ (2008). Combination gemcitabine, platinum, and bevacizumab for the treatment of recurrent ovarian cancer. *Gynecol Oncol* **111**, 461–466.

[31] Kesterson JP, Mhawech-Fauceglia P, and Lele S (2008). The use of bevacizumab in refractory ovarian granulosa-cell carcinoma with symptomatic relief of ascites: a case report. *Gynecol Oncol* **111**, 527–529.

[32] Barrena Medel NI, Herzog TJ, Wright JD, and Lewin SN (2010). Neoadjuvant bevacizumab in a granulosa cell tumor of the ovary: a case report. *Anticancer Res* **30**, 4767–4768.

[33] Vanderhyden BC, Shaw TJ, and Ethier JF (2003). Animal models of ovarian cancer. *Reprod Biol Endocrinol* **1**, 67.

[34] Mullany LK and Richards JS (2012). Minireview: animal models and mechanisms of ovarian cancer development. *Endocrinology* **153**, 1585–1592.

[35] Lague MN, Paquet M, Fan HY, Kaartinen MJ, Chu S, Jamin SP, Behringer RR, Fuller PJ, Mitchell A, Dore M, et al. (2008). Synergistic effects of Pten loss and WNT/CTNNB1 signaling pathway activation in ovarian granulosa cell tumor development and progression. *Carcinogenesis* **29**, 2062–2072.

[36] Nadeau ME, Kaartinen MJ, Lague MN, Paquet M, Huneault LM, and Boerboom D (2009). A mouse surgical model for metastatic ovarian granulosa cell tumor. *Comp Med* **59**, 553–556.

[37] Pautier P, Gutierrez-Bonnaire M, Rey A, Sillet-Bach I, Chevreau C, Kerbrat P, Morice P, Duvillard P, and Lhomme C (2008). Combination of bleomycin, etoposide, and cisplatin for the treatment of advanced ovarian granulosa cell tumors. *Int J Gynecol Cancer* **18**, 446–452.

[38] Brown J, Shvartsman HS, Deavers MT, Ramondetta LM, Burke TW, Munsell MF, and Gershenson DM (2005). The activity of taxanes compared with bleomycin, etoposide, and cisplatin in the treatment of sex cord-stromal ovarian tumors. *Gynecol Oncol* **97**, 489–496.

[39] Pages G, Milanini J, Richard DE, Berra E, Gothie E, Vinals F, and Pouyssegur J (2000). Signaling angiogenesis via p42/p44 MAP kinase cascade. *Ann N Y Acad Sci* **902**, 187–200.

[40] Berra E, Pages G, and Pouyssegur J (2000). MAP kinases and hypoxia in the control of VEGF expression. *Cancer Metastasis Rev* **19**, 139–145.

[41] Qiu Y, Seager M, Osman A, Castle-Miller J, Bevan H, Tortonese DJ, Murphy D, Harper SJ, Fraser HM, Donaldson LF, et al. (2012). Ovarian VEGF$_{165}$b expression regulates follicular development, corpus luteum function and fertility. *Reproduction* **143**, 501–511.

[42] Kaczmarek MM, Schams D, and Ziecik AJ (2005). Role of vascular endothelial growth factor in ovarian physiology—an overview. *Reprod Biol* **5**, 111–136.

[43] Jiang BH and Liu LZ (2009). PI3K/PTEN signaling in angiogenesis and tumorigenesis. *Adv Cancer Res* **102**, 19–65.

[44] Ma J, Sawai H, Ochi N, Matsuo Y, Xu D, Yasuda A, Takahashi H, Wakasugi T, and Takeyama H (2009). PTEN regulates angiogenesis through PI3K/Akt/VEGF signaling pathway in human pancreatic cancer cells. *Mol Cell Biochem* **331**, 161–171.

[45] Borgström P, Bourdon MA, Hillan KJ, Sriramarao P, and Ferrara N (1998). Neutralizing anti-vascular endothelial growth factor antibody completely inhibits angiogenesis and growth of human prostate carcinoma micro tumors *in vivo*. *Prostate* **35**, 1–10.

[46] Inai T, Mancuso M, Hashizume H, Baffert F, Haskell A, Baluk P, Hu-Lowe DD, Shalinsky DR, Thurston G, Yancopoulos GD, et al. (2004). Inhibition of vascular endothelial growth factor (VEGF) signaling in cancer causes loss of endothelial fenestrations, regression of tumor vessels, and appearance of basement membrane ghosts. *Am J Pathol* **165**, 35–52.

[47] Goel S, Duda DG, Xu L, Munn LL, Boucher Y, Fukumura D, and Jain RK (2011). Normalization of the vasculature for treatment of cancer and other diseases. *Physiol Rev* **91**, 1071–1121.

[48] Jain RK (2005). Normalization of tumor vasculature: an emerging concept in antiangiogenic therapy. *Science* **307**, 58–62.

Table W1. Masses of GCTs Used for (A) Immunohistochemistry, Mitotic Figures, TUNEL Assay, Percentage of Necrosis, (B) Tumors from 6-Week-Old Mice Used for Immunofluorescence, and (C) Tumors from 6-Week-Old Mice Used for Western Blot.

(A)

Age (Weeks)	Treatment Received	Tumor Mass (g, Mean ± SEM)
3	–	0.00466 ± 0.000444
4	0.9% NaCl	0.0515 ± 0.00414
4	5 mg/kg anti-VEGFA	0.0618 ± 0.00936
5	0.9% NaCl	0.178 ± 0.0564
5	5 mg/kg anti-VEGFA	0.0830 ± 0.0163
6	0.9% NaCl	0.723 ± 0.258
6	2.5 mg/kg anti-VEGFA	1.08 ± 0.127
6	5 mg/kg anti-VEGFA	0.307 ± 0.151
6	10 mg/kg anti-VEGFA	0.223 ± 0.0485

(B)

Treatment Received	Tumor Mass (g, Mean ± SEM)
0.9% NaCl	1.39 ± 0.238
2.5 mg/kg anti-VEGFA	1.08 ± 0.123
5 mg/kg anti-VEGFA	0.322 ± 0.0223
10 mg/kg anti-VEGFA	0.223 ± 0.0485

(C)

Treatment Received	Tumor Mass (g, Mean ± SEM)
0.9% NaCl	1.39 ± 0.238
2.5 mg/kg anti-VEGFA	1.09 ± 0.127
5 mg/kg anti-VEGFA	0.322 ± 0.0223
10 mg/kg anti-VEGFA	0.223 ± 0.0485